Int. J. Morphol.,
42(3):638-646, 2024.

Effect of Swimming at Low Temperature on Uncoupling Protein Gene Expression in Skeletal Muscle of Wistar Rats

Efecto de la Natación a Baja Temperatura sobre la Expresión del Gen de la Proteína de Desacoplamiento en el Músculo Esquelético de Ratas Wistar

Jinhui Li; Jiaxing Han & Shaoming Yan

LI, J.; HAN, J. & YAN, S. Effect of swimming at low temperature on uncoupling protein gene expression in skeletal muscle of Wistar rats. *Int. J. Morphol., 42(3)*:638-646, 2024.

SUMMARY: As the economy develops and living standards improve, overweight and obesity are increasingly prevalent. Currently, weight-loss medications are primarily administered orally or intravenously, which can result in poor targeting, low bioavailability, frequent administration, and high toxicity and side effects. The study aimed to address these challenges by preparing polylactic acid-polyethylene glycol staple fibers that carry the browning drug pioglitazone hydrochloride using electrostatic spinning and freeze-cutting techniques. Animal experiments were conducted to test the effectiveness of these fibers. Additionally, the study investigated the expression of uncoupling protein genes in rats exposed to different water temperatures by measuring changes in serum urea nitrogen and mRNA expression levels of skeletal muscle uncoupling protein genes. The physiological and genetic effects of low-temperature swimming exercise on changes in energy metabolism in rats were also analyzed at both the individual and molecular levels. The results revealed that serum urea nitrogen remained more stable in hypothermic swimming rats compared to rats in the swimming group. Furthermore, the study observed an induced up-regulation of uncoupling proteins in the skeletal muscle of Wistar rats in response to external temperature stimulation, and the expression of mRNA for skeletal muscle uncoupling proteins significantly increased as the temperature decreased. And the prepared short nanofibers also had a significant promotive effect on uncoupling protein gene, COX7A1, while suppressing the expression of lipogenic gene.

KEY WORDS: Rats; Low Temperature Swimming; UCP Gene Expression; Pioglitazone Hydrochloride; Obesity Treatment.

INTRODUCTION

In recent years, winter swimming has become a popular mass sports program. It is a fitness method that combines cold water bathing, air bathing, and sunbathing, offering a comprehensive approach to disease prevention, fitness, and anti-aging (Jang *et al*., 2021). Winter swimming exercises have shown positive effects in combating obesity by increasing energy expenditure. The exposure to cold environmental stimuli promotes thermogenesis by converting white fat into brown fat, subsequently leading to increased energy expenditure. This process involves the upregulation of uncoupling protein (UCP) expression and an elevated mitochondrial metabolic rate, enabling the conversion of part of the energy that is usually utilized for ATP production into calories (Grace *et al*., 2022). Pioglitazone hydrochloride (PGH) has been found to enhance UCP transcription in human subcutaneous adipocytes and facilitate the function of other mitochondrial proteins involved in the electron transport chain. One highly studied approach in drug delivery is the use of nanoparticles as carriers, particularly for targeted delivery to skeletal muscle tissue (Lingvay *et al*., 2022). Manganese oxide nanoparticles (MnNP) have been widely used in biomedical applications because of their good biocompatibility and high stability and modulability (Kato *et al*., 2021). There is a considerable correlation between type 2 diabetes incidence and obesity. To treat obesity, the study elaborated the effect of low temperature swimming (LTS) on the energy metabolism of the organism by comparing the difference in energy metabolism before and after swimming in Wistar rats under low temperature conditions in terms of changes in Serum urea nitrogen (BUN) and UCP gene expression. Additionally, the study investigated how short fiber-carrying MnNP

College of Physical Education, Qiqihar University, Qiqihar 161000, Helongjiang China.
FUNDED. The research was financially supported by Heilongjiang Province Provincial Universities Basic Research Funds Research Project "Research on the Homology of the Winter Olympics Winter Olympics Projects for Ethnic Minorities in Heilongjiang Province"(project number: 145109162).

Received: 2024-01-17 Accepted: 2024-02-24

synergistic with PGH (SF@PGH-Mn) affected UCP gene expression in skeletal muscle. The aim was to determine the optimal mode of administration and the most effective method of drug loading, thus presenting a novel approach for studying UCP gene expression in skeletal muscle.

MATERIAL AND METHOD

Experimental materials. PELA (Jinan Daigang Biotechnology Co., Ltd., Mw=71.4 kDa); PGH (Tianjin Takeda Pharmaceutical Co., Ltd., purity > 98 %); dopamine hydrochloride (Shanghai Hance Chemical Co., Ltd., purity 98 %); phosphate buffer powder (PBS, Shanghai Kanglang Bio-technology Co., Ltd.); and the commonly used reagents, such as potassium permanganate, oleic acid, ethanol, methylene chloride, N,N- dimethylformamide, trihydroxymethylaminomethane, hydrochloric acid, hydrogen peroxide and potassium pyrophosphate, were purchased from Kermitel Chemicals Co. N,N-, dimethylformamide, trimethylolamine methane, hydrochloric acid, hydrogen peroxide, potassium pyrophosphate, etc. were analytically pure and purchased from Kermitel Chemicals Co. The various instruments used in the experiments and their manufacturers' models are shown in Table I.

Preparation of SF@PGH-Mn. Due to its wide range of spinnable materials, simple manufacturing apparatus, low spinning costs, and regulated process, electrostatic spinning has emerged as one of the primary methods for efficiently preparing nanofiber materials (Shaka *et al.*, 2021). Electrospun fibers prepared by electrospinning technology exhibit excellent mechanical properties, good moisture absorption and air permeability, large porosity, and surface area, as well as good biocompatibility and adjustability. As a result, they have been widely used in various fields including textiles, medicine, and food industry (Duan *et al.*, 2021). Polylactic acid-polyethylene glycol copolymer (PELA) is a highly biocompatible material that is non-toxic, biodegradable, and does not accumulate in vital organs upon degradation (Patel *et al.*, 2020). In the study, PGH was loaded onto PELA oriented fiber membrane by electrostatic spinning method, SF@PGH was prepared by freeze-shearing method, and then MnNP was surface-modified by using polydopamine to obtain SF@PGH-Mn. And Figure 1 depicts the preparation procedure.

The preparation of monodisperse manganese nanoparticles started with precisely weighing 1.0 g of potassium permanganate (6.3 mmol) in 500 mL of ultrapure water, followed by vigorous agitation for thirty minutes. Subsequently, 10 milliliters of oleic acid were added to the reaction mixture, which was then continuously stirred for five hours at 28 °C. The resulting brown precipitate was cleaned with ultrapure water and ethanol successively, and then dried at 80 °C for ten h. The monodisperse manganese nanoparticles were produced by forging in air at 200 °C for 5 h and were subsequently dried in ethanol for the second time.

Accurately weighed 1.0 g of PELA, added a solvent mixture of dichloromethane/N,N-dimethylformamide (mass

Table I. Instrument model and manufacturer.

Name	Manufacturer and model
Clean grade Wistar male rat	Animal Experiment Center, Jilin University
High fat feed	Animal Experiment Center, Jilin University
Ordinary feed	Animal Experiment Center, Jilin University
X-ray diffractometer	Panaco, Netherlands, PertPRO
Fourier transform infrared spectrometer	Nicolet Instruments, USA, Nicolet 5700
With a dynamic light scatterer	Malvern LTD, Nano-ZS90
Scanning electron microscopy	FEI of the Netherlands, QUANTA 2000
Ultraviolet spectrophotometer	Shimadzu Corporation of Japan, UV-2550
Electrophoresis apparatus	Beijing Liuyi Biological Technology Co. LTD, Dycp-31Dn

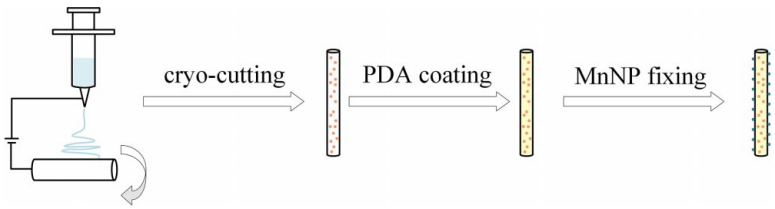

Fig. 1. Preparation flow chart of SF@PGH-Mn.

ratio 5:2), and added PGH at a ratio of 5 % of the polymer loading amount to make a solution with a concentration of 20 % PELA loading. The above mixed solution was injected into a 5 mL plastic injector, and then the injector was fixed in the slot of the microinjector pump for electrostatic spinning, with the propulsion rate set at 0.8 mL/h and the voltage set at 16 kV. The positive output of a high-voltage DC power supply was connected to a metal needle attached to the front end of a syringe. On the receiving end, an aluminum foil was fixed to a grounded drum, with a linear velocity of approximately 15 m/s and a distance of about 15 cm between the needle and the foil, to obtain an oriented fiber film. The resulting fiber film was vacuum dried to remove residual organic solvents, and then placed in ultrapure water and wound parallel to the fibers. After freezing at -20 °C overnight, the film was cut into SF@PGH fibers approximately 20 micrometers in length using a cryo-slicing technique.

To prepare polydopamine-modified SF@PGH-Mn, 20.0 mg of SF@PGH was accurately weighed and added to 10 mL of Tris-HCl buffer (50 mM, pH=8.0). Dopamine was then added to the mixture and stirred under light-avoidance conditions. Polydopamine-modified SF@PGH was prepared by centrifugation, washed in ultrapure water, resuspended in 10 mL of Tris-HCl buffer, 5.0 mg MnNP was added, dispersed by ultrasonication, and stirred for 2 h. Manganese nanoparticles that were not solidly loaded on the staple fibers were separated by low-speed centrifugation to obtain SF@PGH-Mn, which was cleaned in ultrapure water, dried and set aside for use. The SF@Mn preparation process was the same as above.

Characterization of MnNP. The following experimental setup was used in the study to use an X-ray diffractometer (XRD) to determine the crystal structure of MnNP: the X-ray source was CuK@ (incident wavelength λ=0.15406 nm); 40 kV operating voltage; current 20 mA, step width 0.02°, and a scanning range of 2q of 10-70°. A small amount of MnNP was milled into fine particles and then mixed evenly with dried potassium bromide powder. In order to create potassium bromide pressed tablets, the samples were put into a mold for a potassium bromide press. The molds were then placed in an infrared press, and Fourier transform infrared spectroscopy (FTIR) was used to examine the functional group structures. MnNP was added into ultrapure water, and the particle size distribution of MnNP was determined by dynamic light scattering apparatus at 25 °C. MnNP was dispersed in ultrapure water, dropped on a slide, dried, sprayed with gold, and its morphology was analyzed by SEM (Fig. 2).

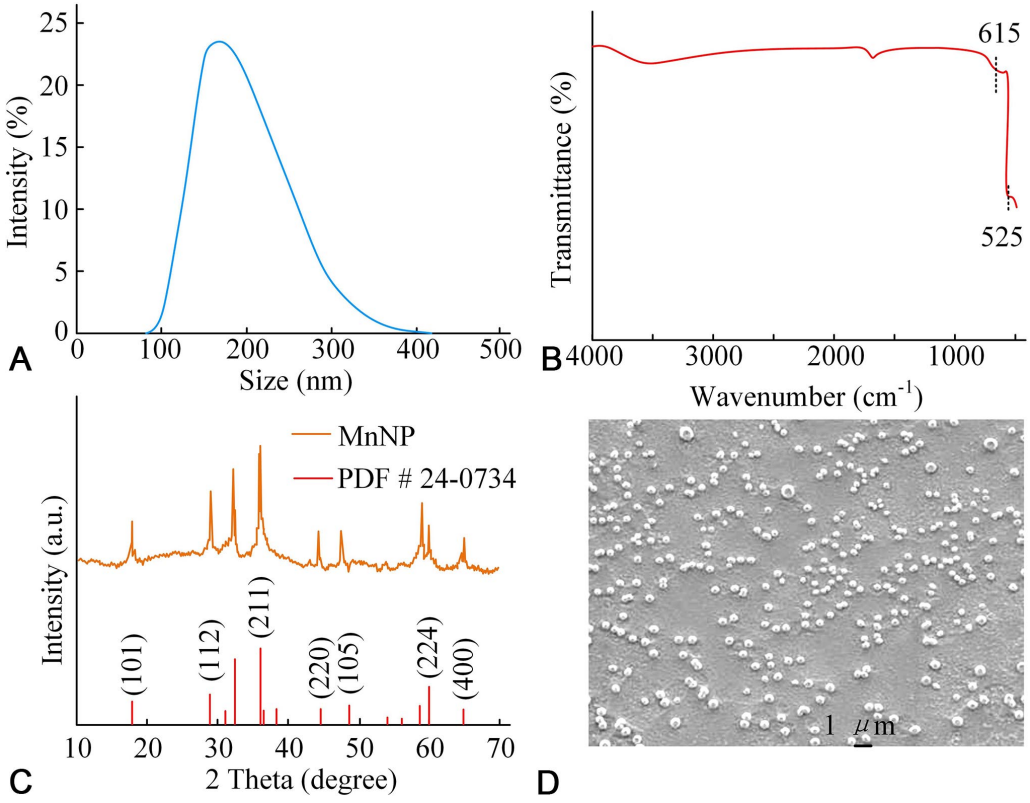

Fig. 2. Characterization of MnNP. (A) Particle size distribution of MnNP. (B) FTIR spectrum of MnNP. (C) XRD pattern of MnNP. (D) SEM diagram of MnNP.

Characterization of SF@PGH-Mn. SF@PGH-Mn was placed in ultrapure water, dropped on a slide, dried and sprayed with gold solution, and its morphology was observed under scanning electron microscope. Additionally, the diameter and length of the samples were ascertained from the obtained SEM pictures using Photoshop 10.0 edition software. The average diameter, average length, and error of the samples were then computed.

To accurately determine the weight of 5 mg of SF@PGH-Mn, it was placed in a 5 mL centrifuge tube. The MnNP on the staple fiber was dissolved using a mixture of dilute hydrochloric acid and hydrogen peroxide. After centrifugation, the supernatant was removed. The resulting solution was then diluted with ultra-high-purity water. Subsequently, 0.6 M and 1 M potassium pyrophosphate-sodium acetate buffers were added. An excess of potassium periodate solution (dissolved in a 1+9 nitric acid solution with a concentration of 20 g/L) was added to oxidize the divalent manganese ions in the solution to purple permanganate. The content of permanganate was measured using UV spectroscopy at an observed wavelength of 525 nm. To obtain the standard curve for MnNP, the appropriate amount of MnNP was weighed and dissolved in a mixture of dilute hydrochloric acid and hydrogen peroxide. Different concentrations of potassium periodate were added for oxidation, and the absorption value at 525 nm was measured. This standard curve was then used as the basis for calculating the actual loading of MnNP.

Low temperature swimming method. Thirty-two clean-grade Wistar male rats weighing 230-280 g were housed in PLA-2 automatic air-feeding cages at a temperature of 24 ± 3 °C and a relative humidity of 40 %-60 %, with free access to food and water, and with lighting that varied according to the natural light in the room. The rats were divided into four groups based on their body weight. The blank control group (Group A) consisted of eight rats, the 5-min swimming exercise group at room temperature (Group B) also had eight rats, the 20-min swimming exercise group at room temperature (Group C) had sixteen rats, and the LTS group (Group D) had eight rats. The LTS-exercised rats in Group D were placed in a homemade swimming tank, with up to eight rats swimming together at a time. The water temperature of the indoor tank was 20 °C in the natural state, and it was lowered by 2 °C per day by using the method of adding ice in the tank, and the water temperature was lowered continuously for one week to 8 °C, and then swimming was continued in the water temperature of 8 ± 1 °C for 7 weeks for 5 min each time. The body weight and basal metabolic rate of the four groups of rats were measured before and after the swimming exercise every day, and the experimental records were made. After participating in a swimming activity, the rats were sampled in the eighth week of the experiment. Eight rats from each of the two groups A and B, C, and D were sampled one day apart, while the remaining eight rats from group C and group D were sampled sequentially. And then the changes in BUN were measured, and the relative UCP gene expression was assessed by analyzing the RNA from the quadriceps muscle of the rats through electrophoresis and RT-PCR reactions (Lingvay *et al*., 2022).

Anti-obesity experiments with SF@PGH-Mn. Fifteen clean-grade Wistar male rats weighing 230-280 g were housed in PLA-2 automatic air-feeding cages at a temperature of 24 ± 3 °C and a relative humidity of 40 %-60 %. After a three-day adaptation period, the rats were divided into two groups: the fat group and the control group. Both groups were monitored for body weight and feeding conditions. The obese group received high-fat foods once every two days, whereas the control group was provided regular diets. After 12 weeks of feeding, rats that were more than 20 % heavier than the regular control group were selected from the obese group for the subsequent anti-obesity test.

Data processing. Tables, line graphs, and data calculations were all done in Excel; data analysis was done with the SPSS program. Group comparisons were performed with a one-way ANOVA. The mean plus standard deviation (Mean ± SD) was used to express all the values. A difference that was significant ($P < 0.05$) or highly significant ($P < 0.01$) was indicated. Amplified fragment size was analyzed by Alpha UV gel imaging system, and optical density analysis of RT-PCR results was performed by Lab words analysis software.

RESULTS

Characterization of MnNP and SF@PGH-Mn. The MnNP characterisation results are displayed in Figure 3. The distribution of MnNP particle sizes is depicted in Figure 3 (A). The distribution of particle sizes falls within the range of 90 to 400 nm, with an average size of 163.25 nm and a dispersion of 0.139. These findings suggest that MnNP homogeneity is satisfactory. Figure 3 (B) shows the FTIR pattern of MnNP, 525 cm^{-1} and 625 cm^{-1} are the stretching vibrations produced by the two bonds of Mn-O and Mn-O-Mn, which belong to Mn_3O_4, respectively. There are broader absorption peaks at 1600-cm^{-1} and 3200-3600 cm^{-1}, and these two broader peaks are the bending vibration and stretching vibration of water molecule and hydrogen-hydrogen bond, respectively. Its peaks at 1300-1500 cm^{-1} and 2800-3000 cm-1 correspond to the carbon-hydrogen bond bending vibration and stretching vibration, and both peaks belong to oleic acid,

indicating that oleic acid is not removed. Figure 3 (C) displays the X-ray diffraction spectrum of MnNP, confirming its composition as tetragonal black manganese ore (JCPDS 24-0734). In Figure 3 (D), the scanning electron micrograph of MnNP particles reveals their uniform size, meeting the requirements of the subsequent experiments.

Figure 3 shows the characterization results of SF@PGH-Mn. Figure 3 (A) and (B) depicts the SEM images of SF@PGH and SF@PGH-Mn. In the figure, SF@PGH has a smooth surface, while SF@PGH-Mn has a large nanoparticles on the surface, which indicates that the surface modification of SF@PGH-Mn by using polydopamine can realize the effective solidification of the material. Software calculations yielded an average particle size of 1.61 ± 0.13 μm and an average length of 19.33 ± 2.25 μm for SF@PGH and yielded an average particle size of 1.90 ± 0.21 μm and an average length of 19.41 ± 1.95 μm for SF@PGH-Mn. The effects of treatment duration and dopamine concentration on PGH and MnNP loading on SF@PGH-Mn are presented in Figures 3 (C) and (D). In Figure 3 (C), the loading of dopamine remains relatively constant after reaching 2 mg/mL within 24 h. Therefore, 2 mg/mL of dopamine was chosen. The loadings of MnNP and PGH on the SF@PGH-Mn surface were 81.63 ± 2.96 μg/mg and 3.13 ± 0.21 %, respectively. Figure 3(D) demonstrates that the loading of PGH gradually decreases as the concentration of dopamine increases, independent of the dopamine content.

Changes in serum urea nitrogen content after completion of exercise training in low temperature swimming. Table II displays the BUN content results following the LTS exercise. The findings revealed that BUN content increased in all groups after training, with a significant difference observed in group A compared to the other groups. Figure 4 illustrates the comparison of BUN content in groups C and D after recovery. Group C exhibited a significantly higher BUN content than group A, while group D showed a BUN content closer to group C than group A, with no significant difference.

Table II. The change of serum BUN.

Group	Sample	Post-training content (mmol/L)	Restore 24-hour content (mmol/L)
A	8	8.26 ± 0.61	/
B	8	10.54 ± 0.78**	/
C	8	12.48 ± 0.67**	9.67 ± 1.01oo
D	8	11.86 ± 0.55**	8.63 ± 0.65

Note. ** means P < 0.01(very significant difference compared with group A) compared with A group; oo indicates P < 0.01(very significant difference compared with group A) compared with A group.

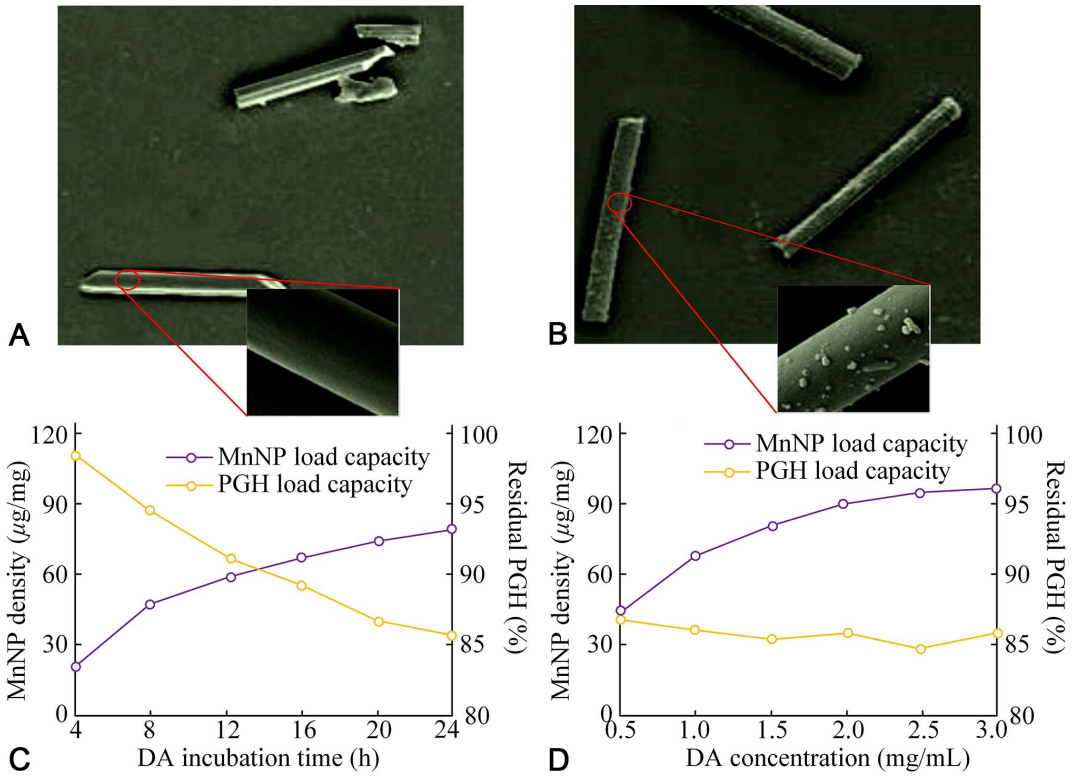

Fig. 3. Characterization of MnNP. (A) SEM image of SF@PGH. (B) SEM image of SF@PGH-Mn. (C) Variation of MnNP and RSG loading with dopamine incubation time at SF@PGH-Mn. (D) Variation of MnNP and RSG loading with dopamine concentration at SF@PGH-Mn.

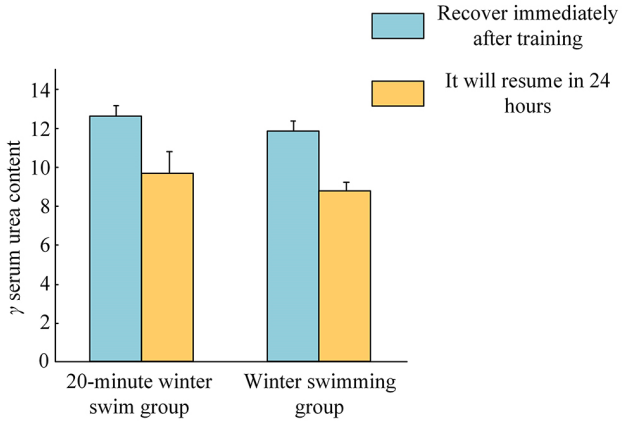

Fig. 4. Compared of serum BUN after 24 h.

Electrophoresis results. The results of electrophoresis of RNA from rat quadriceps deep muscle after completion of swimming training are shown in Figure 5. The results showed three bands of intact 28S, 18S, and 5S RNA, indicating that the RNA samples were intact and not degraded. The results of RT-PCR reaction electrophoresis of UCP gene in deep muscle of rat quadriceps after completion of swimming training are shown in Figure 6. This result showed that the results of relative expression of UCP/b-actin in rat quadriceps after completion of LTS training were clearly visible on the graph, and that the UCP gene was expressed in the muscle tissues of rat quadriceps after completion of LTS training, and the bands were relatively clear and complete, and the fragment size of UCP was analyzed to be about 642 bp.

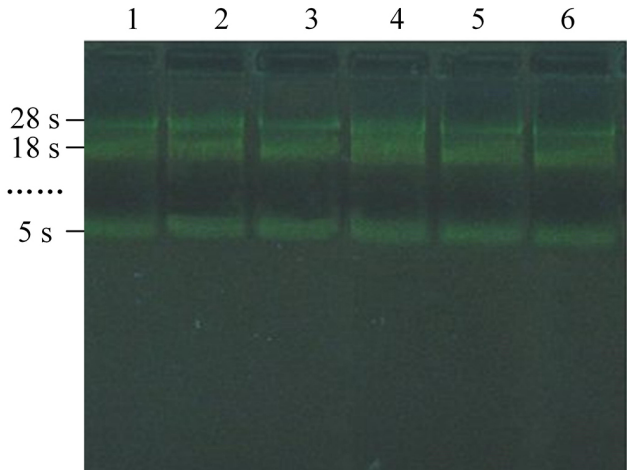

Fig. 5. Results of RNA electrophoresis of quadriceps femoris after swimming training at low temperature. 1: quiet control group; 2: 5 min swimming control group; 3: 20 min swim group; 4: 20 min swim recovery group; 5: Low temperature swimming training group; 6: Low temperature swimming training recovery group.

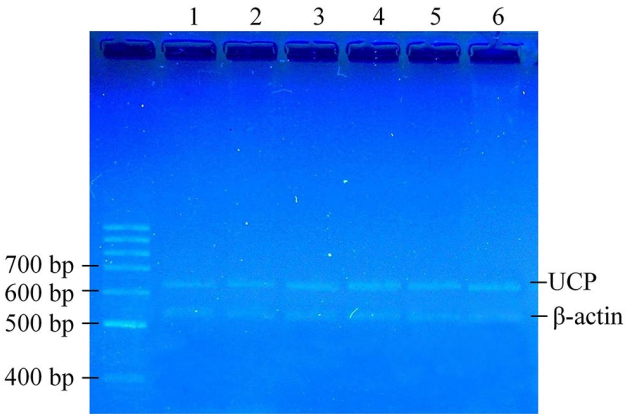

Fig. 6. Results of RT-PCR reelectrophoresis of quadriceps muscles of rats after swimming training at low temperature. 1: quiet control group; 2: 5 min swimming control group; 3: 20 min swim group; 4: 20 min swim recovery group; 5: Low temperature swimming training group; 6: Low temperature swimming training recovery group.

Results of gel density analysis of each band of RT-PCR electrophoresis. The results of RT-PCR electrophoresis of each band of UCP gene in the deep muscle of rat quadriceps after the completion of experimental swimming training showed that the UCP gene could be expressed in the skeletal muscle of rat quadriceps. Additionally, there was a significant increase in UCP mRNA expression in group C and group D compared to group A and group B. Between the 20-min swimming group C and the LTSD group, there was a significantly significant difference in the expression of UCP mRNA level throughout the post-training period. Table III shows the highly significant difference in immediate expression.

Table III. The ratio between intensities of bands corresponding to ucp and internal reference of rat skeletal muscle.

Group	After exercise	24 h after exercise
A Rest control	0.30 ± 0.04	/
B 5 minite exercise	0.54 ± 0.05	/
C 20 minite exercise	0.66 ± 0.16**	0.52 ± 0.12
D Ice exercise	0.73 ± 0.08**oo	0.50 ± 0.23

Note. ** means P < 0.01 (compared with group A and B, the difference is very significant); oo indicates P < 0.01 (very significant difference compared with group C).

According to the results of RT-PCR electrophoresis strip gel density analysis of UCP gene in deep muscle of quadriceps of rats in groups C and D, the data before and after 24 h of swimming recovery were analyzed by Origin for histogram comparison. The results are displayed in Fi-

gure 7. When comparing the UCP mRNA level in the LTS group to the 20 min swimming group, there was a noteworthy upward trend observed, and the difference was statistically significant. Following a 24 h recuperation period, there was no discernible variation in the amounts of UCP mRNA expression between the two groups.

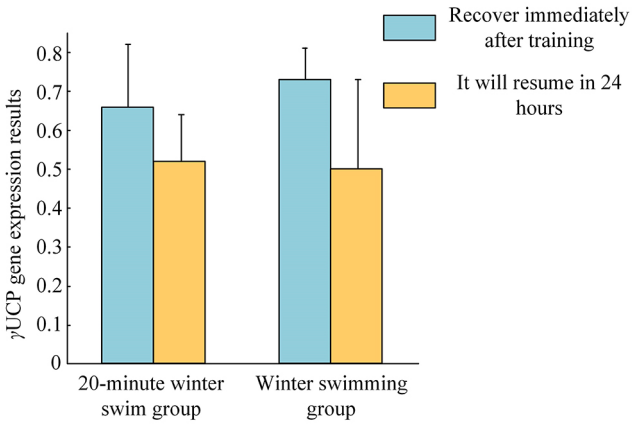

Fig. 7. The relative value of winter/20h in UCPmRNA.

Effect of SF@PGH-Mn on UCP gene expression in skeletal muscle. The browning of white fat is primarily regulated by the protein UCP, which serves as an indirect indicator of browning state (Ceddia *et al*., 2021). COX7A1 is a mitochondrial signature protein that correlates with the number and function of mitochondria, potentially influencing browning. PPARγ is a classical gene regulating fat synthesis, and its down-regulation of expression leads to the decrease of fat-producing function of adipocytes. The study used fluorescence quantitative PCR analysis to detect the RNA expression of different concentrations of short fiber and free drug pairs to reflect the degree of browning and lipid production capacity. Figure 8 shows the quantitative results of UCP, COX7A1, and PPARγ gene expression in each group after short fiber and free drug treatment. As can be seen from Figure 8, SF@PGH and SF@PGH-Mn had significant promotion effects on UCP and COX7A1 ($P < 0.05$), and the effect of SF@PGH-Mn was more obvious ($P < 0.05$), which may be related to the significant inhibitory effect of MnNP on the generation of reactive oxygen species (ROS). SF@PGH, SF@Mn and SF@PGH-Mn significantly inhibited PPARg due to the retention effect of short fibers ($P < 0.05$), and SF@PGH-Mn had the strongest inhibitory effect on promoting the expression of browning genes and inhibition of adipocytes due to the combined effect of PGH and MnNP ($P < 0.05$).

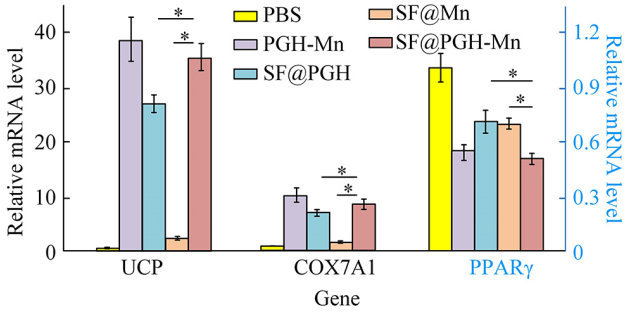

Fig. 8. Quantitative results of UCP, COX7A1 and PPARγ gene expression in each group after treatment with staple fiber and free drug (* represents $P < 0.05$).

DISCUSSION

BUN is a significant product of protein metabolism, serving as an indicator of the body's utilization of protein for energy supply. It indirectly reflects the body's exercise capacity. The primary byproduct of protein metabolism in the body is urea nitrogen (Kato *et al*., 2021). Amino acid deamidation produces NH3, and CO_2, both of which synthesize urea in the liver, and each gram of protein metabolism produces 0.3 g of urea. The experimental results of BUN content after LTS exercise showed that the BUN content increased in all groups compared with group A. The above results indicate that in the process of swimming exercise protein participated in the supply of energy, the protein in the body of rats after exercise to have a certain degree of consumption, protein decomposition into BUN, so the BUN content in the blood of rats in group D group C and group B of the exercise is elevated. Following a 24 h recuperation period, group C's BUN content rose in comparison to group A, with a highly significant difference; in contrast, group D's BUN content was closer to both group C and group A, with a non-significant difference. These findings suggest that group C's rats were physically active. The BUN recovery of rats in group C was slower and did not return to the normal value after 24 h, while the BUN levels of rats in group D returned to the normal value with a moderate amount of exercise.

Cold increases the content and activity of UCP on brown fat mitochondria, and the amount and activity of UCP determines the heat production capacity of BAT. When animals feel cold, the binding of purine nucleotides that inhibit UCP in normal physiological state is lifted, which opens the UCP proton channel and leads to heat production by oxidative phosphorylation uncoupling. To maintain body temperature in a cold environment, more energy is required to be uncoupled through UCP and emitted as heat rather than stored as ATP. UCP genes are involved in the regulation of thermogenesis (Tsuda *et al*., 2021; Fan *et al*., 2022). Experimental findings indicate that rats in groups C and D

exhibited significantly higher levels of UCP gene expression immediately after swimming compared to rats in groups A and B. Moreover, rats in group D showed higher UCP gene expression immediately after LTS than rats in group C. This indicates that swimming exercise can enhance the expression of the UCP gene, and that swimming exercise under cold conditions is more capable of enhancing the expression of the UCP gene. UCP gene expression was significantly enhanced in rats after 8 weeks of LTS training. The amount and activity of UCP play a pivotal role in the body's heat production capacity. When rats are exposed to cold temperatures, the inhibitory effect under normal physiological conditions is lifted, resulting in the opening of the UCP proton channel and subsequent uncoupling of oxidative phosphorylation, leading to heat production. The data obtained from rats in groups C and D returned to the normal expression value of the UCP gene after 24 h of recovery, with no significant difference compared to the other groups of rats. The expression of the UCP gene is regulated by multiple factors, including cold, peroxisomal receptor, T3, retinoic acid (RA), insulin, and glucocorticoids, all of which influence the UCP gene family (El-Beshlawy *et al*., 2021). Animal mitochondrial UCP provides non-shivering thermogenesis and helps animals adapt to cold environments. Cold increases the content and activity of UCP on brown adipose mitochondria, and the amount and activity of UCP determine the thermogenic capacity of brown adipose tissue (BAT). When animals are subjected to cold, the normal physiological state of inhibition of UCP purine nucleotide binding is lifted, so that the UCP proton channel is opened, resulting in heat production by oxidative phosphorylation uncoupling, at the same time, sympathetic excitability is enhanced and the amount of norepinephrine released from the nerve fiber endings is increased, so that BAT and free fatty acids in the skeletal muscle cells are decomposed through the pathway of oxidative phosphorylation uncoupling to produce heat. Under cold environmental conditions, more energy is required to maintain body temperature by uncoupling through the UCP and emitting it as heat rather than storing it as ATP. Rehnmark's induction with cold resulted in a rapid up-regulation of long-pawed gerbil UCP mRNA, followed by a slow decline. Moreover, in the cold, the transcription of brain UCP4 mRNA and UCP5 mRNA increased by 1.5 and 1.7 times, respectively (Frost *et al*., 2020). LTS exercise allows animals to express genes related to cold resistance by initiating their expression (Chen *et al*., 2022), and biological organisms exhibit an increase in basal metabolism or non-shivering thermogenesis after developing cold adaptation. Thermogenesis in animals is an essential physiological function for maintaining body temperature, dispersing excess energy, or as a defense mechanism against infection (Zhu *et al*., 2022). UCP has the potential to uncouple oxidative phosphorylation and plays a crucial role in thermogenesis.

Browning of white adipose tissue (WAT) represents a safe strategy against obesity and related diseases, making it crucial to investigate the mechanisms that facilitate WAT accumulation in beige cells. The expression levels of UCP and COX7A1 in WAT, as browning and mitochondrial marker genes, respectively, can reflect the degree of WAT browning, whereas PPARg, as a typical lipid-forming gene, and its expression level in WAT can reflect the WAT fat-forming ability (Rafeeq *et al*., 2021). Evaluation of the ROS levels and gene expression within rat inguinal WAT revealed that treatment with SF@Rsg-Mn contributed to a reduction in ROS levels in inguinal WAT. Moreover, SF@PGH and SF@PGH-Mn significantly enhanced the expression of browning genes while effectively suppressing lipogenic gene expression, thus leading to significant stimulation of UCP and COX7A1.

CONCLUSION

Obesity is an important causative factor for chronic diseases such as type 2 diabetes, cardiovascular diseases, and cancer. The study was carried out through the controlled release system of anti-obesity drugs and rat LTS experiments, MnNP was prepared by reduction method and heat treatment, SF@PGH was prepared by electrostatic spinning and freeze-cutting technology, and MnNP was immobilized based on the surface modification of polydopamine to obtain SF@PGH-Mn. The relative expression of the UCP gene was evaluated by monitoring changes in BUN levels in the rats, as well as by analyzing the electrophoresis results of deep muscle RNA from the rat tetraspinatus muscle and the RT-PCR electrophoresis results reflecting the relative expression of the UCP gene. The findings demonstrated that the average particle size of SF@PGH was 1.61 ± 0.13 μm, with an average length of 19.33 ± 2.25 μm, and the average particle size of SF@PGH was 1.90 ± 0.21 μm, with an average length of 19.41 ± 1.95 μm. The loadings of MnNP and PGH on the surface of SF@PGH-Mn were 81.63 ± 2.96 μg/mg and 3.13 ± 0.21 %, respectively. The BUN data of LTS rats were more stable than those of rats that underwent 20-minute swimming exercise, and the data of the organism fluctuated less after the exercise, which was more beneficial to the adaptation of the organism compared with the longer swimming exercise at room temperature. UCP gene expression in LTS rats immediately after swimming was significantly higher than in the 20-minute swim group, suggesting that both exercise and temperature can enhance UCP gene expression, particularly when swimming under cold conditions. SF@PGH and SF@PGH-Mn demonstrated noticeable promotion of UCP and COX7A1 expression, with SF@PGH-Mn exhibiting a more pronounced effect. Moreover, SF@PGH-Mn displayed the most effective promotion of browning gene expression and inhibition of

adipocytes due to the combined effects of PGH and MnNP. However, this study still has certain limitations in thoroughly assessing the effects of SF@PGH-Mn and LTS on UCP gene expression in skeletal muscle, calling for future orthogonal experiments to explore the therapeutic effects of obesity using SF@PGH-Mn combined with LTS.

Ethical Compliance. The experimental procedure follows the "Guidelines for Ethical Review of Animal Experiment Welfare" of the Science and Technology Ethics Committee of Qiqihar University.

LI, J.; HAN, J. & YAN, S. Efecto de la natación a baja temperatura sobre la expresión del gen de la proteína de desacoplamiento en el músculo esquelético de ratas Wistar. *Int. J. Morphol., 42(3)*:638-646, 2024.

RESUMEN: A medida que la economía se desarrolla y los niveles de vida mejoran, el sobrepeso y la obesidad son cada vez más frecuentes. Actualmente, los medicamentos para bajar de peso se administran principalmente por vía oral o intravenosa, lo que puede resultar en una mala focalización, baja biodisponibilidad, administración frecuente y alta toxicidad y efectos secundarios. El estudio tuvo como objetivo abordar estos desafíos mediante la preparación de fibras cortadas de ácido poliláctico y polietilenglicol que transportan el fármaco pardo clorhidrato de pioglitazona mediante técnicas de hilado electrostático y liofilización. Se realizaron experimentos con animales para probar la eficacia de estas fibras. Además, el estudio investigó la expresión de genes de proteínas desacopladoras en ratas expuestas a diferentes temperaturas del agua midiendo los cambios en el nitrógeno ureico sérico y los niveles de expresión de ARNm de genes de proteínas desacopladoras del músculo esquelético. También se analizaron los efectos fisiológicos y genéticos del ejercicio de natación a baja temperatura sobre los cambios en el metabolismo energético en ratas, tanto a nivel individual como molecular. Los resultados revelaron que el nitrógeno ureico sérico permaneció más estable en ratas nadadoras hipotérmicas en comparación con las ratas del grupo de natación. Además, el estudio observó una regulación positiva inducida de las proteínas desacopladoras en el músculo esquelético de ratas Wistar en respuesta a la estimulación de la temperatura externa, y la expresión de ARNm para las proteínas desacopladoras del músculo esquelético aumentó significativamente a medida que disminuía la temperatura. Además, las nanofibras cortas preparadas también tuvieron un efecto promotor significativo sobre el gen de la proteína de desacoplamiento, COX7A1, al tiempo que suprimieron la expresión del gen lipogénico.

PALABRAS CLAVE: Ratas; Natación a baja temperatura; Expresión del gen UCP; Clorhidrato de pioglitazona; Tratamiento de la obesidad.

REFERENCES

Ceddia, R. P.; Liu, D.; Shi, F.; Crowder, M. K.; Mishra, S.; Kass, D. A. & Collins, S. Increased energy expenditure and protection from diet-induced obesity in mice lacking the cGMP-specific phosphodiesterase PDE9. *Diabetes, 70(12)*:2823-36, 2021.

Chen, B.; Cai, H.; Mao, C.; Gan, Y. & Wei, Y. Toughening and rapid self-healing for carbon fiber/epoxy composites based on electrospinning thermoplastic polyamide nanofiber. *Polym. Compos., 43(5)*:3124-35, 2022.

Duan, X.; Sun, W.; Sun, H. & Zhang, L. Perfluorooctane sulfonate continual exposure impairs glucose-stimulated insulin secretion via SIRT1-induced upregulation of UCP2 expression. *Environ. Pollut., 278*:116840, 2021.

El-Beshlawy, M. M.; Abdel-Haleem, F. M. & Barhoum, A. Molecularly imprinted potentiometric sensor for nanomolar determination of pioglitazone hydrochloride in pharmaceutical formulations. *Electroanalysis, 33(5)*:1244-54, 2021.

Fan, M.; Zhang, X.; Zhao, Y.; Zhi, J.; Xu, W.; Yang, Y.; Xu, Y.; Luo, K. & Wang, D. Mn(ii)-mediated self-assembly of tea polysaccharide nanoparticles and their functional role in mice with type 2 diabetes. *ACS Appl. Mater. Interfaces, 14(27)*:30607-17, 2022.

Frost, P. A.; Chen, S.; Rodriguez-Ayala, E.; Laviada-Molina, H. A.; Vaquera, Z.; Gaytan-Saucedo, J. F.; Li, W. H.; Haack, K.; Grayburn, P. A.; Sayers, K.; *et al*. Research methodology for in vivo measurements of resting energy expenditure, daily body temperature, metabolic heat and non-viral tissue-specific gene therapy in baboons. *Res. Vet. Sci., 133*:136-45, 2020.

Grace, C.; Hopewell, J. C.; Watkins, H.; Farrall, M. & Goel, A. Robust estimates of heritable coronary disease risk in individuals with type 2 diabetes. *Genet. Epidemiol., 46(1)*:51-62, 2022.

Jang, J.; Chang, S. H.; Song, D.; Song, N. J.; Han, S.; Oh, S.; Yun, U. J.; Ahn, J. Y.; Lee, S.; Ku, J. M.; *et al*. Butein-enriched fractions of Butea monosperma (Lam.) Taub. flower decrease weight gains and increase energy expenditure in high-fat diet-induced obese mice. *J. Med. Food., 24(12)*:1271-9, 2021.

Kato, H.; Ario, T.; Kishida, T.; Tadano, M.; Osawa, S.; Maeda, Y.; Takakura, H. & Izawa, T. Homeobox A5 and C10 genes modulate adaptation of brown adipose tissue during exercise training in juvenile rats. *Exp. Physiol., 106(2)*:463-74, 2021.

Lingvay, I.; Sumithran, P.; Cohen, R. V. & le Roux, C. W. Obesity management as a primary treatment goal for type 2 diabetes: time to reframe the conversation. *Lancet, 399(10322)*:394-405, 2022.

Patel, B. V.; Yao, F.; Howenstine, A.; Takenaka, R.; Hyatt, J. A.; Sears, K. E. & Shewchuk, B. M. Emergent coordination of the CHKB and CPT1B genes in eutherian mammals: implications for the origin of brown adipose tissue. *J. Mol. Biol., 432(23)*:6127-45, 2020.

Rafeeq, C. M.; Paul, E.; Saagar, E. V. & Ali, P. P. M. Mycosynthesis of zinc oxide nanoparticles using Pleurotus floridanus and optimization of process parameters. sciencedirect. *Ceram. Int., 47(9)*:12375-80, 2021.

Shaka, H.; Wani, F.; El-Amir, Z.; Dahiya, D. S.; Singh, J.; Edigin, E.; Eseaton, P. & Kichloo, A. Comparing patient characteristics and outcomes in type 1 versus type 2 diabetes with diabetic ketoacidosis: a review and a propensity-matched nationwide analysis. *J. Investig. Med., 69(6)*:1196-200, 2021.

Tsuda, Y.; Matsuyama, A.; Makihara, K.; Higaki, K.; Motoi, T.; Okuma, T. & Hisaoka, M. Nuclear expression of MDM2 in hibernoma: a potential diagnostic pitfall. *Virchows Arch., 478(3)*:527-34, 2021.

Zhu, Y.; Wang, K.; Lu, J.; Pan, Z.; Rong, J.; Zhang, T.; Yang, D.; Pan, J. & Qiu, F. Teamed boronate affinity-functionalized Zn-MOF/PAN-derived molecularly imprinted hollow carbon electrospinning nanofibers for selective adsorption of shikimic acid. *ACS Appl. Mater. Interfaces*, 2022. DOI: https://www.doi.org/10.1021/acsami.2c06664

Corresponding author:
Jinhui Li
College of Physical Education
Qiqihar University
Qiqihar 161000
Helongjiang
CHINA

E-mail: jinhuili654@outlook.com